



OPEN

Short-term analysis of urban noise dynamics during covid-19 lockdown using a machine learning approach in Mashhad, Iran

Raheleh Valizadeh Ardalan¹, Mitra Mohammadi¹✉, Mohammad Sadegh Bahadari², Mandana Mohammadi³, Seyed Mohammad Mahdi Moezzi⁴ & Didem Saloglu⁵✉

Noise pollution is an important environmental issue that has a significant effect on human health. This study investigates the short-term impact of human activities on noise pollution in the Mashhad, Iran, and how these patterns changed during the COVID-19 pandemic. By leveraging a dual strategy, a comprehensive analysis was initiated. First, the equivalent continuous sound level (L_{eq}) measurements collected before (March 21 to April 20, 2019) and during (March 20 to April 19, 2020) the COVID-19 quarantine period at four key intersections in Mashhad were compared. The non-parametric Wilcoxon signed-rank test was employed to evaluate the statistical significance of the observed changes. The results showed a statistically significant reduction in L_{eq} at all four intersections during the quarantine period. Next, a predictive modeling algorithm named random forest (RF) was developed to predict noise pollution levels by considering time factors such as month, day, hour, and cumulative hour. The RF model achieved a high R-squared (R²) value (0.914), representing a strong correlation between predicted and actual L_{eq}. The predictive power of this model was demonstrated by the root mean square error (RMSE) of 0.967 and the mean absolute error (MAE) of 0.620, indicating reasonable accuracy. This case study demonstrates evidence that human activities are the main cause of noise pollution in Mashhad. The findings highlight the potential benefits of urban planning strategies that reduce traffic and noise generation. Furthermore, developing of a noise prediction model using a random forest approach provides a practical solution for future noise management efforts at the local scale.

Keywords Noise pollution, COVID-19, Lockdown measure, L_{eq} changes, Wilcoxon signed-rank test, Random forest

Urban landscapes are places full of noise and activity and alongside this commotion, there is a hidden problem¹. Noise pollution is a major urban environmental problem, and reducing it improves quality of life and public health². The continuous increase in traffic, urbanization, industrialization, and infrastructure development in and around cities are the main sources for the growing problem of noise pollution in metropolitan areas. 75% of total noise pollution in urban areas is caused by the combined effects of the commercial, industrial, and transportation sectors³. Noise exposure has been proved to have significant and persistent negative human health effects⁴. The importance of understanding noise pollution and its sources within urban settings is highlighted by their health impacts⁵. Exposure to noise pollution can lead to adverse health effects such as increased aggression, physical and mental fatigue, heightened stress, feelings of dizziness, headaches, irritability, distraction, disruption of sleep patterns, cardiovascular diseases, children's cognitive, auditory system, obesity, and decreased efficiency in work performance⁴⁻¹⁰. According to Tiwari et al. (2022), mental health symptoms including headache and hypertension are significantly affected by noise pollution¹¹. In another study, Patel et al. (2024b) emphasized the need for comprehensive noise management approaches using structural equation modeling to demonstrate that noise annoyance and sensitivity directly affect human health outcomes¹². As stated by Patel et al. (2024a),

¹Department of Environmental Sciences, Kheradgarayan Motahar Institute of Higher Education, Mashhad, Iran.

²Department of Civil Engineering, Technical University of Lisbon, Lisbon, Portugal. ³Research and Development Unit, AirpaajCo, Mashhad, Iran.

⁴Department of Civil Engineering, Sharif University of Technology, Tehran, Iran.

⁵Department of Disaster and Emergency Management, Disaster Management Institute, Istanbul Technical University, 34469 Istanbul, Turkey. ✉email: mitramohammadi@gmail.com; saloglu@itu.edu.tr

there are serious concerns about human health related to traffic noise, highlighting the need for accurate noise prediction models to enable effective urban noise reduction strategies¹³.

The year 2020 presented a unique opportunity to investigate the relationship between human activity and noise pollution. The global response to the COVID-19 pandemic, with the widespread implementation of lockdown measures, significantly altered the structure of daily life in cities worldwide^{14,15}. Movement restrictions and lockdowns significantly impacted human activity, transportation, and urban noise levels worldwide, leading to broad decreases in traffic, industrial operations, and intercity travel^{15–20}. Understanding how these changes impact environmental noise has become a key topic in recent studies. The pandemic offers a unique opportunity to assess the effectiveness of public health policies to reduce human activities and the resulting environmental pollution, including noise^{21,22}. Although limited studies have been conducted in this field in Iran, other environmental indicators, including noise, have been widely studied globally during the pandemic. Mishra et al. (2021) explored the impact of COVID-19 lockdown measures on changes in noise levels across residential, commercial, industrial, and quiet zones in Kanpur, India, before, during, and after the lockdown period¹⁰. While noise levels declined significantly in commercial zones during the lockdown, all other monitored areas exceeded India's Central Pollution Control Board's recommended noise thresholds. Similarly, Joshi and Pakhrial (2021) examined noise pollution in Dehradun, a Himalayan city, during lockdown, noting that noise levels across monitoring stations dropped well below the 60 dB standard²³. Basu et al. (2021) analyzed data from 12 sound measurement stations in Dublin, Ireland. Their statistical analysis revealed significant reductions in noise levels due to traffic movement restrictions during lockdown²⁴. Rumpler et al. (2021) employed statistical analysis and linear regression on sound sensor data in a crowded place in Stockholm, Sweden from mid-April 2019 to the end of June 2020²⁵. Despite a few limitations in government measures during the pandemic, their study indicated a decrease in noise levels. In another study, Munoz et al. (2020) analyzed sound data from 21 continuous monitoring stations across five towns in southern France throughout the lockdown period. They compared these measurements with pre-lockdown values. Results indicated a decrease in noise levels from 6 to 4 dB in settlements situated near busy roads²⁶. Although these studies provide useful information about noise levels changes under quarantine conditions, it remains unclear how such changes occur in cities with specific characteristics and challenges, such as Mashhad, Iran.

Mashhad, located in the northeast of Iran, is at the center of this research. As a major pilgrimage center that attracts millions of visitors annually, Mashhad has witnessed an increase in human activities compared to many Iranian cities²⁷. Crowded streets, filled with people and vehicles, undeniably contribute to increasing ambient noise levels²⁸. However, the urban landscape of Mashhad underwent a significant transformation during the COVID-19 pandemic. The strict quarantine measures imposed in March 2020 led to a significant reduction in street-level human activity. This temporal shift provided a valuable opportunity to explore the relationship between human presence and noise pollution^{22,29}. Therefore, this research aimed to investigate the impact of COVID-19 quarantine on urban equivalent continuous sound level (Leq) in Mashhad city. To achieve this goal, a dual strategy combining statistical analysis and machine learning method was employed. The primary strategy involved comparing Leq measured before (March 21 to April 20, 2019) and during (March 20 to April 19, 2020) the COVID-19 quarantine period. This direct comparison, using the Wilcoxon signed-rank test, allows us to evaluate statistically significant changes in Leq resulting from the implementation of lockdown measures. The Wilcoxon signed-rank test was chosen for its suitability for paired data and its robustness in dealing with potentially non-normally distributed data such as noise pollution data. Using this test, reliable statistical findings were obtained by determining whether the observed fluctuations in Leq over the two time periods are statistically significant or simply the result of chance. This approach is in line with previous studies that have successfully used the Wilcoxon signed-rank test to assess changes in noise levels and other environmental factors during the COVID-19 outbreak. For example, Caraka et al. (2021) and Velastegui-Montoya et al. (2023) used this test to analyze noise levels in Taiwan and Guayaquil, Ecuador, respectively^{30,31}. Additionally, other researchers have utilized this test to analyze other environmental factors, such as hospital noise³², subjective noise responses³³, and human perception of environmental sounds³⁴. These studies demonstrate the ability of the Wilcoxon test to analyze paired data, specifically skewed data that is often present in environmental studies^{32–34}. It is worth noting that, the present study is the first to use the Wilcoxon signed-rank test to investigate urban noise pollution in Mashhad during the COVID-19 quarantine period, providing important information about the impact of reduced human activities on the city's soundscape.

In the second approach, a powerful machine learning method, random forest (RF) algorithm was used to create a noise-level forecasting model. Machine learning methods such as RF and support vector regression perform excellently in analyzing complex environmental noise patterns due to their ability to recognize nonlinear relationships between noise levels and other environmental influencing factors^{35–40}. In particular, RF has shown great potential in this area. Liu et al. (2020)³⁶ showed superiority of RF over traditional methods for noise estimation, while Liu et al. (2021)³⁷ employed RF to develop high-resolution noise maps. Fan and Signorelli (2024) successfully applied RF to predict repeat noise complaints to highlight the wide application potential of RF⁴¹. Moreover, the strength of RF in analyzing complex environmental datasets, including noise and temporal data in diverse contexts like COVID –19 pandemic has been demonstrated in studies like Ren et al. (2024)⁴², and Manzella et al. (2021)⁴³. Unlike previous studies, the present research develops the RF model by utilizing temporal factors such as month, day, hour, and cumulative hours, as well as the pre-lock noise measurements. This approach provides a new way to capture the short-term effects of human activity patterns on noise pollution dynamics during the COVID-19 lockdown period. By combining these factors, the RF model can learn complex patterns and relationships that traditional methods may ignore. The effectiveness of this model will be evaluated based on its performance metrics, such as R-squared (R^2), mean absolute error (MAE) and root mean squared error (RMSE).

This localized case study contributes to the limited knowledge about noise dynamics in developing countries by analyzing noise pollution in Mashhad during the COVID-19 quarantine. The main motivation of this research is the need to understand changes in Mashhad's urban soundscape after the COVID-19 pandemic by implementing machine learning techniques. While this study focuses on a specific context, it provides valuable insights by analyzing the relationship between human activities, urban environments, and environmental quality during a period of significant social change. As a regionally focused case study, its findings provide practical recommendations for local urban planners and policymakers to develop effective noise management strategies and improve the acoustic environment for residents in similar urban settings.

Materials and methods

This section provides an overview of the methods used to analyze the impact of COVID-19 quarantine on urban noise pollution levels in Mashhad, Iran. It begins by discussing study area, station selection and data acquisition, and then describes the Leq measurement equipment at fixed monitoring stations. Subsequently, a statistical approach using the Wilcoxon signed-rank test is employed to assess the differences in Leq before and during the quarantine. Furthermore, a machine learning approach is introduced, where a RF model is developed to predict Leq based on pre-lockdown data and temporal factors. Hyperparameter tuning and model evaluation criteria are presented at the end of this section. The complete workflow of this study adapted from Das et al. (2021)⁴⁴ showing the step-by-step methodology from data collection to analysis and prediction. This workflow is presented in Fig. 1 to provide a clear visual understanding of the process.

Study area

Mashhad is the capital of Razavi Khorasan province in northeastern Iran, with coordinates of 36°16'N and 59°38'E. The map of Mashhad and the location of monitoring stations in this metropolis are shown in Fig. 2. Mashhad is Iran's second most populous city after Tehran. According to the 2014 census, Mashhad, covering about 315 square kilometers, had a population of around 3,001,184. Notably, owing to the existence of the shrine of the 8th Shiite Imam, the city annually hosts over 30 million visitors⁴⁵.

(Fig. 2a) was created using QGIS software version 3.40.3 (<https://qgis.org>) with administrative boundary data sourced from the GADM database- GADM's licensing terms can be accessed directly at: <https://gadm.org/license.html>; Fig 2b,c were created by OpenStreetMap data (accessed May 2025, <https://www.openstreetmap.org/#map=4/39.03/35.25>) and Python program (version 3.12.7.).

Station selection and data acquisition

Noise pollution data were obtained from the Urban Pollutants Monitoring Center of Mashhad Municipality, which is in charge of city-level environmental surveillance. Although, five fixed sound monitoring stations have been installed in the city of Mashhad by this center, only 4 of which were selected during the study period. These stations include 15 Khordad Square, Chaman-Mosalla Intersection, Mofatteh-Tabarsi Intersection, and Shohada Intersection, all of which are located at key urban intersections (Fig. 2 and Table 1). The main criterion for selecting these stations was the completeness and reliability of the data, which is essential for valid comparative analysis. Pre-pandemic data from some stations were restricted due to equipment failures, power outages, calibration issues, and inadequate infrastructure. Furthermore, geopolitical restrictions and sanctions limited access to advanced noise monitoring equipment, replacement parts, and analytical tools impacting data quality and long-term research efforts. Particularly, two monitoring sites (Chaman-Mosalla Intersection and Mofatteh-Tabarsi Intersection) lacked complete full year pre-pandemic data, limiting the analysis to the March–April 2019 period, when data collection was more consistent. Accordingly, for reliable comparative analysis, an equal one-month March–April 2020 duration time frame for pandemic has been chosen.

Aside from data quality concerns, the stations were chosen based on their strategic urban importance and land-use representation. The surrounding environment within a 1-km radius of each station was taken into account, given the influence of land use on noise pollution. This allows the present study to effectively capture the initial patterns of noise changes in Mashhad's urban fabric during the lockdown. Table 1 includes information on industrial zones, airports, railroads, commercial centers, and construction activities. Table 2 also provides a summary of the geographical coordinates of major intersections in Mashhad. As Table 1 explains, the selected intersections are located in mixed-use areas that include administrative, religious, transportation, and commercial-residential areas. Even though this study does not cover all land use types in Mashhad, such as purely industrial zones or suburban residential areas, the selected typology still reflects the city's main urban patterns. Thus, the chosen intersections can be considered representative of the primary urban fabric that generates noise under both normal and lockdown conditions. This targeted selection aligns with international best practices in urban environmental research. Recent COVID-19 lockdown studies have similarly focused on monitoring noise levels in high-traffic areas, city centers, and major intersections to better capture changes caused by lockdowns. These studies found that the greatest reductions in noise occurred in these high-traffic and central areas, while changes in low-traffic or suburban areas were significantly smaller. This demonstrates the scientific value of well-chosen monitoring locations^{20,24,46,47}. The complete hourly Leq datasets for every monitoring station during the pre-lockdown and lockdown periods are provided in Supplementary File 1.

Leq measurement equipment at fixed monitoring stations

At the study stations, a NOR140 sound level meter equipped with a NOR1216 microphone, manufactured by Norsonic (Norway) was used to measure noise levels. This device complies with EPA and WHO standards (ANSI S1.4 for sound level meters and IEC 61672 Class 1 for noise measurement equipment). It was capable of measuring sound levels across a dynamic range from 15 dB to 137 dB, with options for 1/1 and 1/3 octave

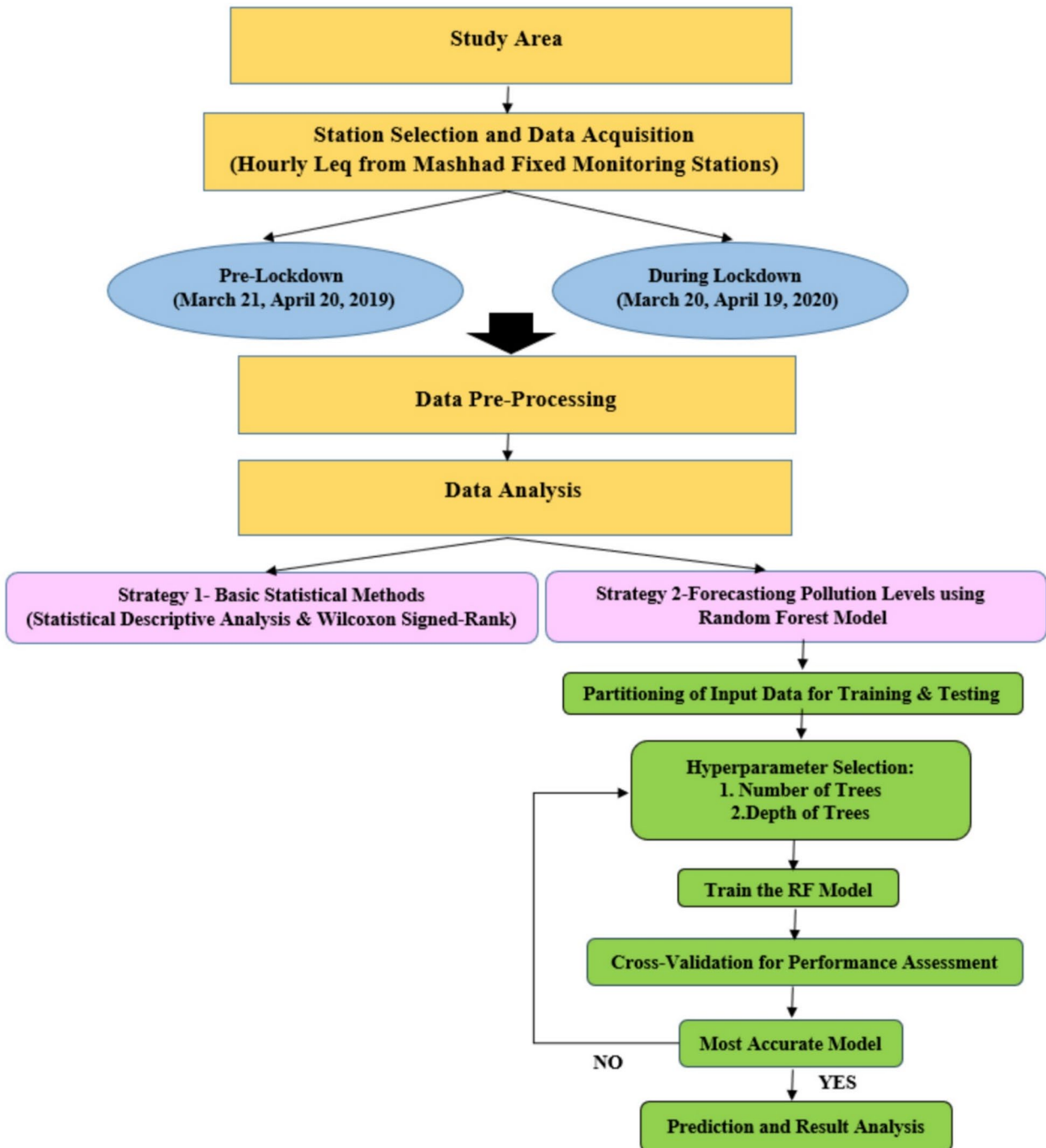


Fig. 1. The study framework to assess the influence of covid-19 lockdown measures on noise pollution in Mashhad.

frequency bands (0.4 Hz to 20 kHz). For this study, the system was set up with an A-weighted frequency network, fast response speed, and a frequency range of 30–130 dB for hourly noise measurements.

According to WHO guidelines (1999), microphones should be placed 1.2 to 1.5 meters above the ground and at least 3.5 meters away from reflective surfaces. However, in this study, to address several key concerns, the microphones were positioned 4 meters above the ground at the fixed monitoring stations, rather than at the 1.2–1.5 meters recommended by WHO (1999). These concerns include contamination from intermittent human and vehicular movement, minimizing the impact of ground-level reflections, capturing a stable, integrated environmental noise signature at busy intersections, and reducing potential interference from nearby structures or activities. While the microphones' placement in this study differs from WHO's (1999) guidelines, other international standards such as ISO 1996-2:2017, Acoustics – Description, measurement and assessment of environmental noise – Part 2 allow for adjustments in microphone height to improve measurement accuracy

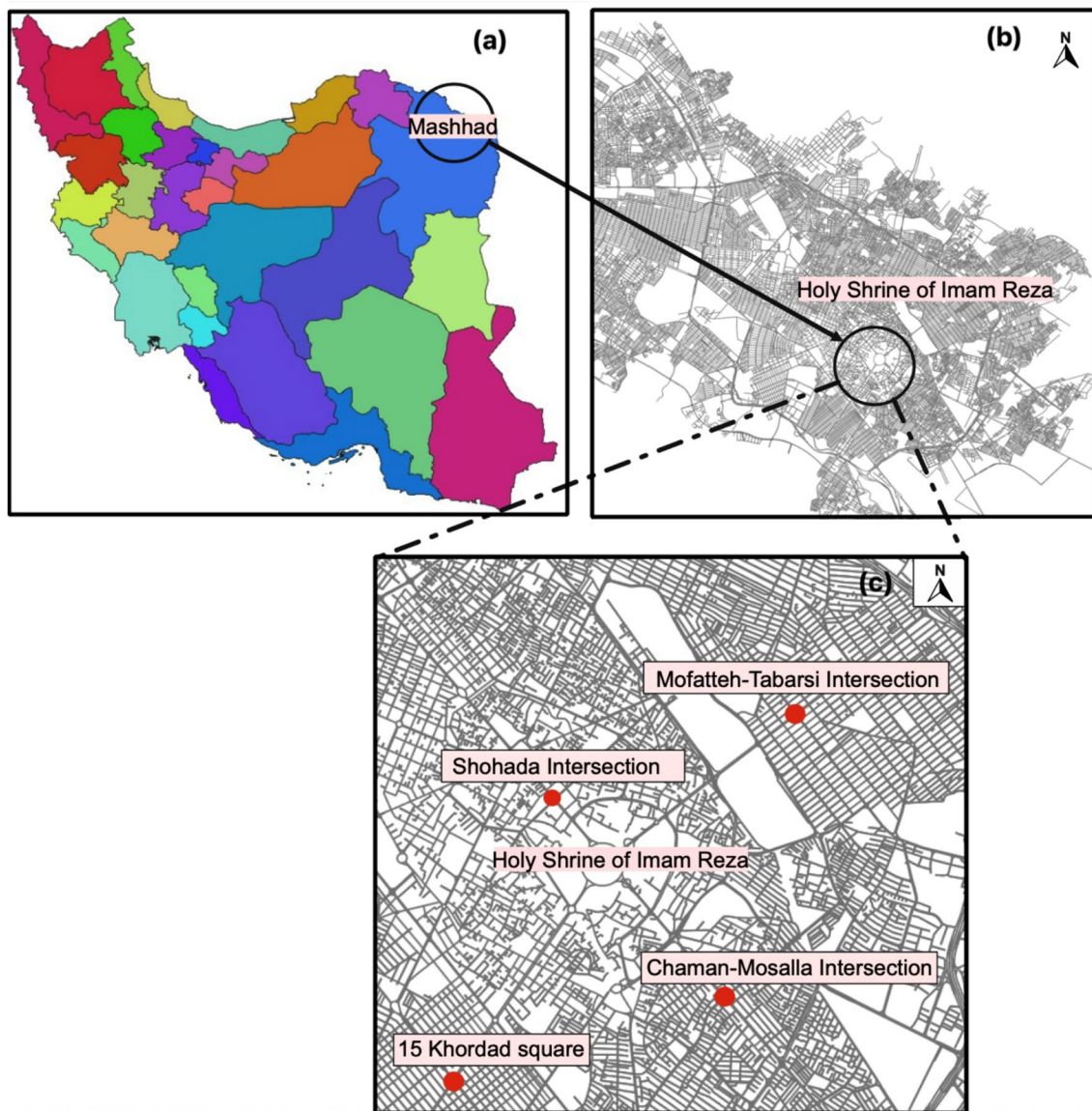


Fig. 2. Study area and location of monitoring stations (Source: created by authors).

in challenging urban environments⁴⁸. Similarly, the U.S. Environmental Protection Agency (EPA, 1974) permits microphone positioning up to 5 meters in complex urban settings to capture a more stable and representative ambient sound level⁴⁹. Mashhad's fixed sound monitoring stations are located at the city's main intersections, which are frequently characterized by high levels of vehicular and pedestrian traffic, a lot of commercial activity, and numerous reflective surfaces (like storefront windows, traffic signs, billboards, and parked cars), all of which deviate from the ideal conditions assumed in WHO's (1999). In such an environment, placing microphones at 1.2 to 1.5 meters apart increases exposure to short-distance, low-level transient noise and ground reflections, creating significant measurement errors (such as transient, reflective, and interfering noises). Studies such as Caraka et al. (2021), Rumpler et al. (2021), and Gonzalez et al. (2020) have shown that selecting a higher microphone placement (e.g., 4 meters) helps to minimize these effects and improves measurement accuracy in urban settings^{25,30,50}.

The microphone sensor was further protected from air currents and weather conditions using an absorbent sponge. Fig. 3 shows the measurement setup and surrounding environment at fixed sound measurement stations. It should also be noted that no significant background noise from particular sources was present at any of the stations, as this factor was carefully considered during the site selection process. However, rainfall occurred on March 20–22, 2020, which might have had a minor impact on the recorded Leq.

Instruments were calibrated before each monitoring period using a Class 1 acoustic calibrator (94 dB at 1000 Hz), following IEC 60942 and the manufacturer's instructions. Post-measurement calibration checks confirmed the instrument's stability and showed no significant drift. The estimated combined measurement uncertainty

Number	Land Use Type	Station name			
		15 Khordad square	Chaman-mosalla intersection	Moffatreh-tabarsi intersection	Shohada intersection
		Area (square meters)			
1	Residential	1,463,311.00	1,362,322.09	719,712.00	1,275,854.00
2	Administrative	77,880.00	4,643.00	111,941.00	40,882.00
3	Educational	104,218.00	132,947.00	67,805.00	87,597.00
4	Commercial-residential	33,434.00	868.00	11,436.00	93,286.00
5	Commercial	167,274.00	39,990.00	24,821.00	110,995.00
6	Religious	34,447.00	-	-	23,316.00
7	Medical-healthcare	43,582.00	14,634.00	16,830.00	28,814.00
8	Recreational-sports	452,701.00	143,616.00	16,627.00	26,160.00
9	Hotel-guest house	1,595.00	-	-	5,484.00
10	Tourist-hospitality	12,954.00	-	-	1,597.00
11	Municipal facilities	57.00	-	-	758.00
12	Transportation and warehousing	9,999.00	-	69,734.00	5,701.00
13	Agricultural	-	-	-	93.00
14	Green space	2,854.00	-	-	9,423.00
15	Cultural-historical	64,308.00	8,095.00	1,657.00	-
16	Unspecified	13,707.00	235,969.00	13,814.00	242,199.00
17	Other	18,714.0	352.00	495,422.00	-

Table 1. Existing land use area within a 1000-meter radius of static sound emission stations in mashhad city (source: mashhad municipality urban pollutant monitoring center).

Station name	X coordinate	Y coordinate
15 Khordad Square	733,452.297	4,016,854.629
Chaman-Mosalla Intersection	736,193.717	4,017,728.706
Moffatreh-Tabarsi Intersection	736,484.193	4,020,351.634
Shohada Intersection	734,400.988	4,019,727.537

Table 2. Geographical coordinates of major intersections in Mashhad, Iran.

(device accuracy, environmental conditions, and microphone positioning) was below ± 1 dB which is consistent with accepted environmental noise monitoring limits.

The device was set to record sound levels automatically at regular intervals. Data acquired included essential characteristics such as Leq, maximum sound levels (Lmax), and minimum sound levels (Lmin). Leq represents the average sound energy over a specified period, which is used as the primary metric for assessing environmental noise. To preprocess the recorded noise data, Norsonic's software was used to extract the data from the NOR140 device and export it into Excel format. A sample output file from the sound level meter, along with the instrument's technical specifications, is provided in Supplementary Files 2 and 3.

Data analysis

Strategy 1- Wilcoxon signed-rank test

To compare the levels of noise pollution before and during the lockdown, a preliminary comparative analysis was conducted. A non-parametric substitute for the paired t-test - the Wilcoxon signed-rank test- was therefore used to determine whether or not the variations in Leq between these periods were statistically significant. Each monitoring station produced 1,426 paired data points by providing 713 hourly Leq measurements for the pre-lockdown month and 713 for the during-lockdown month, ensuring no missing data during the analysis period, validated the usage of the Wilcoxon signed-rank test for all stations. In order to avoid artificial bias, the Wilcoxon signed-rank test was performed using only reliable and uninterrupted measurements, without any extrapolation or imputation.

Prior to comparative analysis, the Shapiro-Wilk test of normality was assessed to show significant deviations from normality ($p < 0.05$) across all datasets. This test is necessary to confirm the application of the Wilcoxon signed-rank test as a non-parametric approach. Other nonparametric tests, such as the Mann-Whitney U test are not appropriate for the paired measures in this study because they are made for independent samples. The Wilcoxon signed-rank test compares the means of two dependent groups at a significance level of 5%. Equation (1) provides the test statistic Z for the Wilcoxon signed-rank test, where n is the reduced sample size, excluding any differences of zero.



Fig. 3. Measurement and surrounding environment at fixed sound measurement stations.

$$Z = \frac{\left(WS - \frac{(n(n+1)}{4} \right)}{\sqrt{\frac{n(n+1)(2n+1)}{24}}} \quad (1)$$

WS denotes the smaller in absolute value of the signed ranks for a two-tailed test, the sum of the positive ranks for a left-tailed test, or the sum of the negative ranks for a right-tailed test⁵¹.

Strategy 2- Random forest model

The second strategy for predicting noise pollution levels was to use a Random Forest regression model. This method is widely used in ensemble machine learning because it is highly effective at predicting continuous numerical values. RF was selected as the modeling method due to its ability to handle large datasets, its robustness against overfitting, and its suitability for time-structured environmental data⁵². These qualities, especially its capacity to handle complex relationships between the output variable and its features, make it a suitable option for estimating noise pollution³⁷. Furthermore, it has been shown to perform better than land use regression models in capturing the spatial variability of noise levels³⁶. An RF regression model creates multiple decision trees by randomly selecting features and subsets from the dataset. Each tree produces a separate forecast, and the final result is calculated by averaging the outputs of all the trees⁵³. Fig. 4 provides an illustration of how an RF model integrates multiple decision trees to generate a final prediction for a given input. The RF model utilized in this study was developed using Python and the scikit-learn library, which provides robust capabilities for developing and evaluating models. To enhance data presentation, Excel was utilized to produce clear and understandable graphics.

In the past, RF models have been widely employed for environmental forecasting, including the prediction of noise pollution and air quality^{36,54–56}. These studies show how RF models are suitable for handling complex environmental data, such as those analyzed in this paper, and how well they manage such data. Although RF is widely used in environmental modeling, this study did not aim to present a novel machine learning approach. Instead, RF was used as a baseline to capture noise patterns before the COVID-19 lockdown. The model was trained on pre-lockdown data using only temporal variables, which allowed it to capture typical noise patterns. Deviations from this baseline during the lockdown period were then analyzed as evidence of behavioral and mobility changes, rather than as forecasting errors per se. In this context, RF was not used as a forecasting tool but rather served as a diagnostic tool to detect changes in urban activity patterns during lockdown. Further modeling details of RF are described in the next subsection.

Data preprocessing and modeling details

We first meticulously preprocessed the historical Leq data to ensure data quality and improve the RF model's forecast accuracy. During this step, the data were screened to identify and eliminate any inaccurate readings that

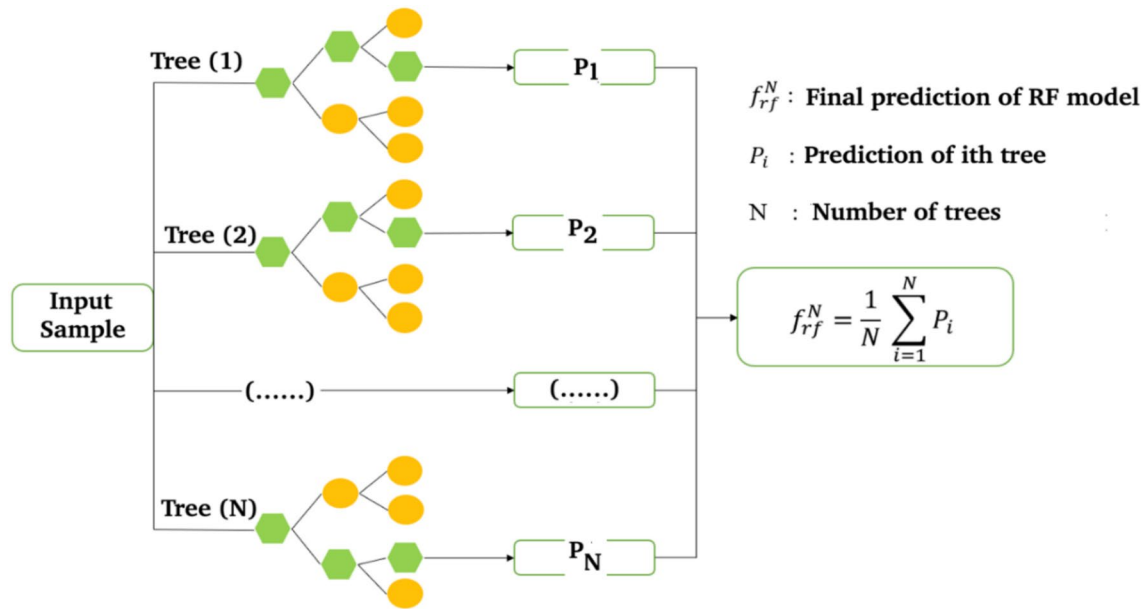


Fig. 4. Integration of multiple trees within the random forest algorithm.

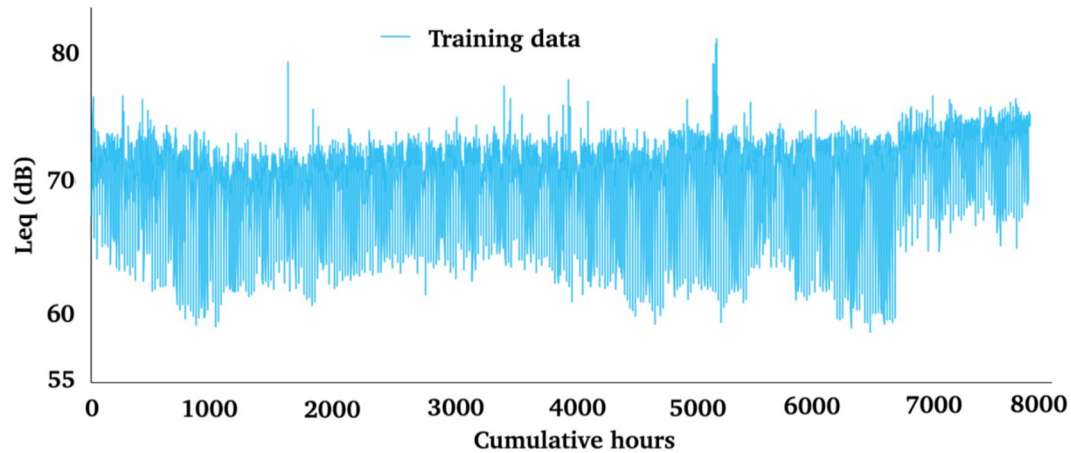


Fig. 5. Training data used for implementation of random forest model.

might have been caused by equipment malfunctions, unexpected environmental disturbances, or power outages. The statistical techniques were used to identify and eliminate outliers, such as abnormally high or low Leq inconsistent with normal environmental conditions. We identified and removed outliers using the Interquartile Range (IQR) method. Specifically, we considered the values outside of the range of $Q1 - 1.5 \times IQR$ to $Q3 + 1.5 \times IQR$ ($Q1$ and $Q3$ represent the 25th and 75th percentiles, respectively) as outliers⁵⁷. This resulted in the removal of approximately 0.33% of the total data points, a negligible amount that does not affect the representativeness or statistical integrity of the dataset. Following common practice in time-series research, we removed these outliers and imputed missing values using the mean of the neighboring data points¹⁵. This cleaning process ensured that the percentage of missing and omitted data for the entire Leq dataset remained below 1%. Fig. 5 illustrates how data from almost a year before the lockdown was used to train the RF model. The Leq values ranged from 58.8 dB to 80.8 dB, with an average of 70.47 dB.

To effectively analyze how Leq changed before and during the COVID-19 lockdown, we chose to focus our modeling on the Shohada monitoring station. This decision was based on both the quality and completeness of its data. Compared to other stations, Shohada provided the most reliable and consistent dataset. It included 7,820 hourly Leq measurements, covered a longer period than that used for the Wilcoxon test, and had very few missing values. In contrast, the other stations had substantial gaps—especially in the critical pre-lockdown period—making them unreliable for modeling. Although we considered using imputation techniques to fill in missing values, the extent and pattern of missingness at these stations were too irregular and exceeded acceptable thresholds, which could have compromised the validity of our results. As a result, we prioritized using high-

integrity data from a single, dependable source over including more locations with weaker datasets. Beyond its data quality, the Shohada station is located in a busy urban district near the Imam Reza Holy Shrine, an area known for constant human activity, even during times of restricted movement. This made it a particularly insightful setting to assess the impact of lockdowns on urban noise, especially in a place where reductions might be less pronounced. Focusing on one high-quality station also allowed us to maintain a consistent and coherent analysis, minimizing variability and strengthening the overall reliability of our findings. The decision to use Shohada station was, therefore, not only practical but also methodologically sound and aligned with the goals of this study.

Although traffic volume, weather, and mobility data are known to influence urban noise levels, these variables were intentionally excluded from the RF model to maintain the counterfactual framework of this study. In this context, a counterfactual framework simulates a hypothetical scenario in which pre-lockdown conditions continued uninterrupted. The RF model was exclusively trained on pre-lockdown data, collected from March 21, 2019, to March 19, 2020, using temporal input features such as month, day, hour, and cumulative hour, with Leq as the target output. This setup was designed to simulate noise level predictions during the first ten days of lockdown period (March 20 to March 30, 2020) based on the assumption that temporal patterns remained consistent. The model architecture was intentional, as our goal was to establish a baseline of pre-pandemic patterns, not to develop a general-purpose model for predicting noise under different conditions. Although we did not include traffic volume, weather, or mobility data as features, this decision was consistent with our modeling strategy. This design ensures that the observed discrepancy between predicted and actual Leq values serves as indirect evidence of the lockdown's effect on noise independent of short-term variations such as weather.

The ability of the RF model to predict Leq values was examined by using walk-forward time-series cross-validation with an expanding training window and a fixed validation horizon of 73 days (20% of the pre-lockdown period). In this setup, the model was trained on all available data up to the day before each validation window and tested on the subsequent 73 days, with the window advancing by 12 days in each of ten folds. After completing cross-validation, the model was retrained on the entire pre-lockdown dataset and used to generate counterfactual predictions for the lockdown period (March 20–30, 2020).

To avoid data leakage and ensure the model predicted future values based on historical patterns, we kept the data in its original chronological order. The average performance metrics across all iterations provided a reliable assessment of the model's overall performance. We also developed a simpler linear regression model, using the same time-based inputs, to predict Leq levels as a baseline for comparison. This comparison tested whether the RF model, which captures complex patterns, outperformed the simpler linear regression model.

Hyperparameter tuning and model training

We improved the RF model's performance using time-series cross-validation and hyperparameter tuning. This procedure required careful adjustment of key hyperparameters affecting the model's learning, including the number of trees (`n_estimators`), the maximum depth of each tree (`max_depth`), and the random seed (`random_state`). To increase the model's prediction accuracy and generalizability, the goal was to identify the optimal parameter configuration for the dataset.

The number of trees in the RF model is determined by `n_estimators` option. More trees generally result in more accurate predictions, but they also need more processing power. Each tree's maximum depth is set by the `max_depth`, which helps to balance catching intricate patterns in the data with lowering the chance of overfitting. Setting a fixed `random_state` ensures reproducibility and enables the model to produce consistent outcomes during several rounds¹⁵.

We achieved the model's optimal configuration by carefully adjusting the hyperparameters across a number of iterations. We assessed performance using time-series cross-validation, which preserves the chronological order of the data. This method sequentially separates the dataset into training and validation sets while maintaining its temporal structure, ensuring that the model is tested on unseen data with time-based patterns similar to real-world scenarios. This approach provides a trustworthy assessment of the model's ability to generalize to new data, particularly for datasets with temporal dependencies.

Table 3 presents the final configuration of the RF model, determined through hyperparameter tuning and time-series cross-validation. Evaluating performance on temporally consistent data subsets significantly enhanced the model's predictive accuracy while reducing the risk of overfitting.

Model evaluation metrics

We evaluated the effectiveness of the optimized RF model in predicting Leq using three common performance measures: MAE, RMSE, and R² Table 3. These measures, described by Equations (2 - 5), numerically assess how closely the model's predictions align with observed noise pollution data. Each metric provides unique insight into model performance.

Random forest hyperparameters	Value
<code>n_estimators</code>	1000
<code>max_depth</code>	100
<code>random_state</code>	50

Table 3. Final Random Forest Models Hyperparameters.

The coefficient of determination, or R^2 , expresses how much of the variance in observed values (y) can be explained by the model's predictions (f). Higher R^2 values, up to 1, signify a better match between the model and the observed data. Here, y is the observed or real data, f is the predicted data that came from the model, n is the total number of data points that were utilized for validation, and \bar{y} is the observed data's overall mean⁵⁸.

$$R^2 = 1 - \frac{SS_{residual}}{SS_{total}} \quad (2)$$

$$SS_{residual} = \sum_i (y_i - f_i)^2, SS_{total} = \sum_i (y_i - \bar{y})^2 \quad (3)$$

The RMSE measures the average difference between the expected and actual Leq by squaring the errors, averaging them, and then taking the square root. Squaring is vulnerable to outliers since it magnifies greater errors. On the other hand, the MAE computes the average of the absolute discrepancies between predictions and actual values, ignoring their direction. Since MAE does not require squaring the errors, it is less vulnerable to outliers and provides a more robust measure when the data contains extreme values⁵⁸.

$$MAE = \frac{1}{n} \left(\sum_i |y_i - f_i| \right) \quad (4)$$

$$RMSE = \sqrt{\frac{1}{n} \left(\sum_i (y_i - f_i)^2 \right)} \quad (5)$$

Results and discussion

This section presents a detailed examination of the research findings. We examined the Leq from pre-lockdown and lockdown period, using descriptive statistics. Furthermore, we compared noise pollution indices between these two periods at each monitoring station using the Wilcoxon signed-rank test. The results of the RF model used to predict Leq changes during the COVID-19 lockdown, are analyzed in the second part.

Descriptive statistics and statistical analysis

Table 4 presents the hourly Leq for the four monitoring stations from pre-lockdown and lockdown period, using descriptive statistics. The total number of Leq measurements taken at each station during each period is 713. The statistics show that the average hourly Leq in March-April 2019 ranged from 71.13 dB at the 15 Khordad Square station to 69.18 dB at the Moffatreh-Tabarsi station. All stations exceeded Iran's Environmental Protection Organization's threshold of 60 decibels for commercial-residential zones. Notably, the Moffatreh-Tabarsi station had the lowest average hourly Leq in both 2019 and 2020, while the highest values were found at the 15 Khordad and Shohada intersection stations (Table 4). However, these values still exceeded the permitted limit.

These findings are similar to previous studies conducted in Iran by Emamjomeh et al. (2010)⁵⁹, Moasher et al. (2012)⁶⁰, and Yari et al. (2016)⁶¹, which emphasized the persistent problem of noise pollution in cities.

The violin plots were created to visualize the distribution of Leq at each monitoring station

(Fig. 6). Side-by-side violin plots complemented the descriptive statistics in Table 4 for examining the impact of the COVID-19 lockdown on noise pollution levels in Mashhad. These plots represent the distribution of Leq at each intersection. Wider sections of the violin plots indicate higher noise density, whereas narrower sections suggest lower probability. Python, along with libraries such as Matplotlib and Seaborn, was used to generate the plots. Furthermore, Excel was utilized to further process and refine the visual representation of the data.

Violin plots show several important observations. Notably, the quartiles (dotted lines at Q1 and Q3) and the median (dashed line) for all four intersections appear to be lower during the lockdown period compared to the pre-lockdown period. For example, the average Leq in 15 Khordad Square station decreased from 71.13 dB before the lockdown to 70.65 dB during the lockdown. This indicates a possible decrease in Leq citywide as a result of less human activity during the lockdown. Moreover, violin plots offer a way to gain insight into

Station name	Time frame	Statistical measures			
		Mean	Std. deviation	Minimum	Maximum
15 Khordad square	Pre-lockdown	71.13	3.49	60.20	81.80
	Lockdown	70.65	3.42	60.46	78.03
Chaman-mosalla intersection	Pre-lockdown	70.02	3.67	58.70	77.60
	Lockdown	69.19	2.93	60.37	75.69
Moffatreh-tabarsi intersection	Pre-lockdown	69.18	3.50	57.80	75.50
	Lockdown	65.23	3.91	53.29	73.10
Shohada intersection	Pre-lockdown	70.48	2.768	61.90	76.50
	Lockdown	70.40	2.769	61.82	76.34

Table 4. Hourly Leq amount in April 2019 and 2020 in four study intersections.

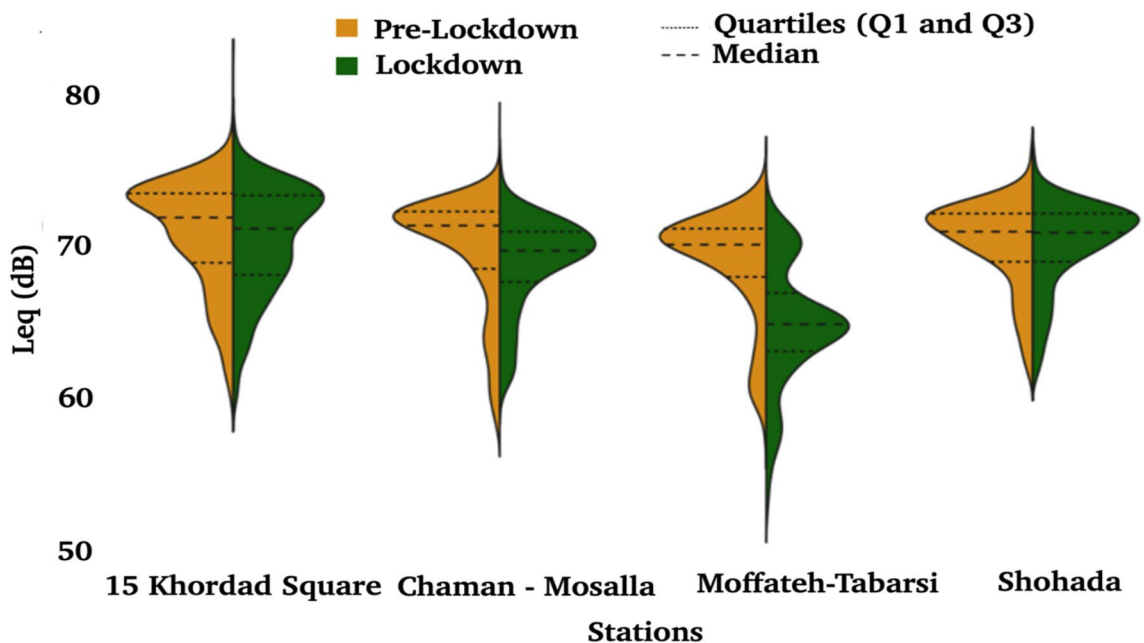


Fig. 6. Violin plots of leq at monitoring stations.

Station name	Time frame	Shapiro-Wilk		
		Statistic	df	Sig
Chaman-mosalla intersection	Pre-lockdown	0.815	713	0.000
	Lockdown	0.905	713	0.000
15 Khordad square	Pre-lockdown	0.836	713	0.000
	Lockdown	0.959	713	0.000
Moffateh-tabarsi intersection	Pre-lockdown	0.836	713	0.000
	Lockdown	0.959	713	0.000
Shohada intersection	Pre-lockdown	0.901	713	0.000
	Lockdown	0.901	713	0.000

Table 5. The Shapiro-Wilk Normality Tests of Leq at Various Monitoring Sites in Mashhad in 2019 and 2020.

fluctuations in Leq. In some cases, narrower violin plots are observed during the lockdown period compared to the pre-lockdown period. This could suggest a reduction in Leq during lockdown, indicating a more consistent noise environment.

The Wilcoxon signed-rank test, a nonparametric statistical test, was used to assess the statistical significance of observed differences in Leq between two periods. By examining the descriptive statistics, interpreting the violin charts, and performing the Wilcoxon signed-rank test, we can comprehensively understand the impact of reduced human activities on the noise pollution levels of Mashhad.

Wilcoxon signed-rank test

We conducted the Shapiro-Wilk test for each station and period to assess the normality of the hourly Leq distributions (sample size $n = 713$ per group). The results revealed the significant deviations from normality across all stations ($p < 0.05$), justifying the use of Wilcoxon signed-rank test as a non-parametric method. For instance, the pre-lockdown period at the 15 Khordad Square, had $W = 0.836$ ($p < 0.001$), while the lockdown period had $W = 0.959$ ($p < 0.001$). Other intersections showed similar results, with all p values less than 0.05 (Table 5).

The Wilcoxon signed-rank test was utilized to compare hourly Leq between the pre-lockdown and lockdown periods at each monitoring station. The results revealed a statistically significant difference in Leq between these periods at all four monitoring stations ($p < 0.05$). This significance is evident from the Asymptotic Significance (Asymp. Sig.) values in Table 6, which are all less than 5%. Moreover, the confidence intervals, at 95% for the difference in Leq between the two time frames do not include zero (refer to Table 6), providing additional evidence for this conclusion.

In general, the findings suggest that the average Leq at all stations in April 2020 (during the COVID-19 lockdown) was considerably lower than during the same period in 2019 (before the lockdown). In particular,

Test statistics ^a	Station			
	15 Khordad square	Chaman-mosalla intersection	Moffatteh-tabarsi intersection	Shohada intersection
Z	-8.449	-11.473	-19.815 ^b	-22.795 ^b
Asymp. Sig. (2-tailed)	0.000	0.000	0.000	0.000

Table 6. The Wilcoxon signed-rank test of leq at various monitoring sites in Mashhad in 2019 and 2020. a Wilcoxon signed rank test. b Based on positive ranks

decreases in Leq were seen at Moffatteh-Tabarsi (3.95 dB), Chaman-Mosalla (0.83 dB), 15 Khordad (0.48 dB), and Shohada (0.08 dB) intersections (Table 4). The reduction in noise from traffic during the pandemic and lockdowns aligns with research conducted in Rome⁶², Argentina⁶³, and Stockholm⁶⁴.

Nonetheless, the Shohada intersection had the smallest reduction in Leq compared to the other stations. The noise reduction at this intersection may result from its proximity to both Imam Reza Shrine and Shohada Square (a main square of the city), located about 500 meters away. Concern about contracting COVID-19 within the middle to upper-middle-class population likely led to a shift from public transport to private vehicle use during the lockdown. Eight out of thirteen urban areas in Mashhad have strong communities located near the city center and the Imam Reza Shrine. Therefore, even though the shrine is closed, residents can still drive their own cars for pilgrimage, which will reduce the Leq at the Shohada intersection. In addition, the closure of hotels and guest houses near the shrine may not lead to a significant reduction in Leq. Local residents may have rented accommodations to pilgrims, resulting in continued activity and a slight reduction in noise compared to other stations. This finding aligns with Rumpler et al. (2021) who found that noise reduction was lower on weekends compared to weekdays²⁵.

Despite the decreases noted, the average Leq at all stations during April 2020 (lockdown period) still surpassed the permissible limit of 60 dB set by the Iranian Environmental Protection Agency for residential-commercial areas (Table 4). Different environmental factors contribute in this continuous noise pollution. Some factors are weather conditions (such as rain and strong winds in early April 2020), narrow roads (like Shirazi Street near Shohada Square), poor asphalt quality (seen at most stations), absence of vegetation (particularly in Chaman-Mosalla and Moffatteh-Tabarsi), crowded buildings, and commercial hubs (like Shohada intersection). These findings are consistent with the research of Alsina-Pags et al. (2021) and Rodríguez et al. (2022)^{64,65}.

In summary, the COVID-19 lockdown led to a notable decrease in noise pollution levels at every monitoring site. Nevertheless, these decreases were insufficient to lower Leq below the allowable threshold. Given the influence of different environmental factors, additional measures are required to eliminate noise pollution in Mashhad.

Random forest model performance

Following validation using a time series cross-validation technique with 10 folds and an 80% training size, the RF model performed well. The average R^2 value for these folds was 0.914, with a standard deviation of 0.013. This result indicates a well-tuned and precise model capable of capturing the underlying relationships within the data. Also, the RF model's feature importance analysis revealed that "hour" had the highest relative importance (0.750), followed by "cumulative hour" (0.199), "day" (0.039), and "month" (0.012). This indicates that short-term diurnal cycles had the strongest correlation with Leq values. The high accuracy of the model (average $R^2 > 0.914$, low RMSE and MAE) confirms valid and statistically significant results of this study even with a short-term focus.

Although the study period was limited to March–April of 2019 and 2020, the purpose of the study was to examine short-term noise changes during the COVID-19 lockdown rather than the long-term seasonal patterns. This period served as a natural experiment, allowing the evaluation of Leq variations by time-related factors (month, day of the week, hour) under exceptional conditions. Despite the short time frame the dataset included 7820 hourly Leq observations which is considered a sufficient and reliable volume for machine learning analysis. Furthermore, 10-fold time series cross-validation maintained temporal regularity, prevented data leakage, and provided a robust estimate of model performance.

These findings support the validity and scientific relevance of our approach, and confirm the model's ability to capture significant patterns from data even with the limited time frame. This short-term approach is also consistent with studies such as Asensio et al. (2020)²⁰, Basu et al. (2021)²⁴, and Ahmed et al. (2021)⁶⁶.

Fig. 7 visualizes the model's performance on a single validation fold. The red points represent predicted values for unseen data by the final RF model, while the blue line represents all training data. As shown in the figure, the RF model accurately forecasts unseen data points. In addition to the time series prediction shown in Fig. 7, residual analysis was performed to evaluate the distribution of prediction errors. Fig. 8 presents the residual plot, which illustrates the relative difference between predicted and actual Leq values for the same validation fold. The vertical axis shows the residual percentage, calculated as $(\text{Predicted} - \text{Actual})/\text{Actual} \times 100$, while the horizontal axis corresponds to the index of each data point. The residuals are centered around zero with no strong pattern or bias, further confirming that the RF model performs consistently across different time segments and does not exhibit systematic over- or under-prediction. Moreover, the scatter plot of actual vs. predicted values is shown in Fig. 9. In this figure, the blue dots represent the predicted values, and the red line represents the trend line. If the predicted values are closer to the line, it indicates that the predictions are more accurate.

The linear regression model's results, obtained using the same methods, showed significant variability (standard deviation 0.633) and an average R^2 close to zero (-0.0254), underscoring its inability to capture the

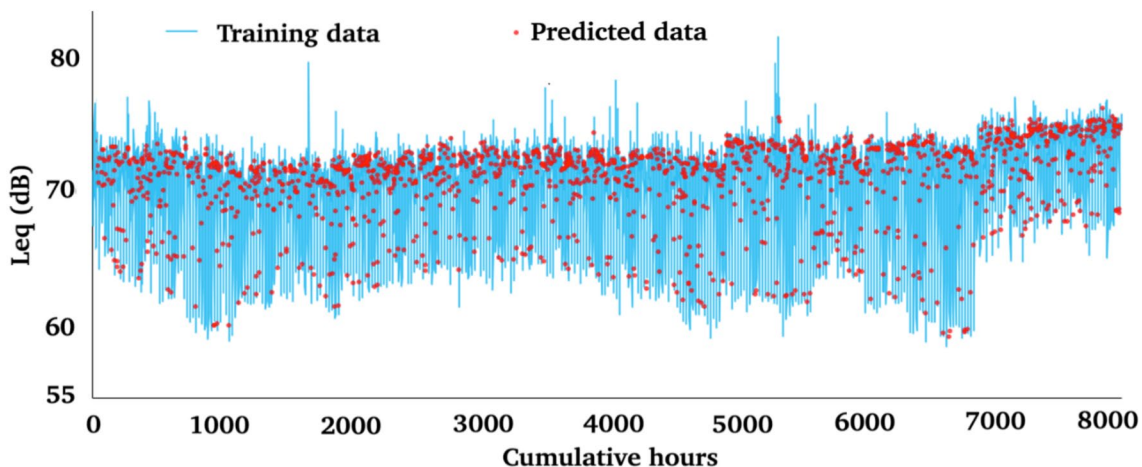


Fig. 7. Random forest prediction of leq for one cross-validation subset.

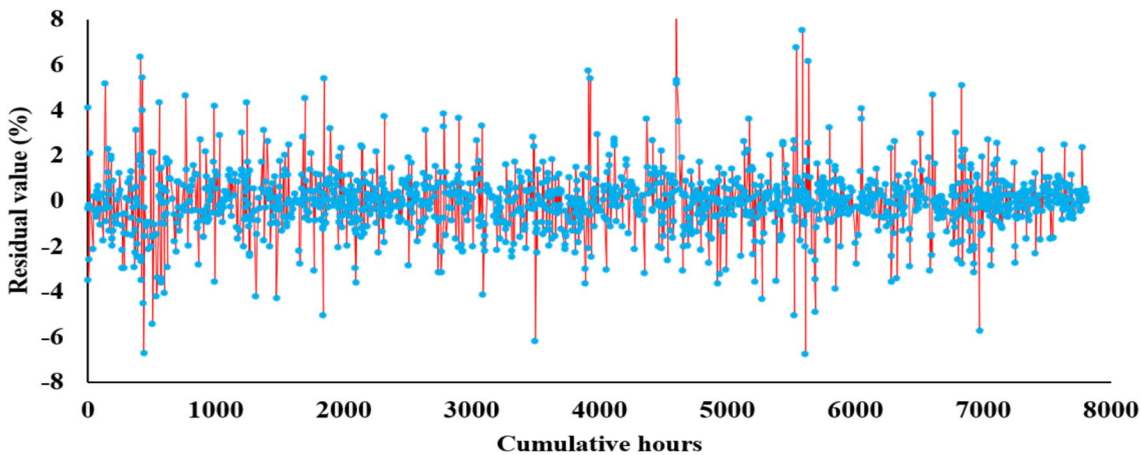


Fig. 8. Visualization of residuals for random forest predictions on the same validation subset used for performance evaluation.

complex and non-linear interactions between the predictors and the target variable. However, the RF model, by employing multiple decision trees, successfully captured these intricate patterns and achieved a significantly higher R^2 value. This enhanced ability to generalize to unseen data shows how effective the RF model is for real-world prediction applications.

Forecasting noise pollution during lockdown

After validating the model's accuracy, it was used to forecast Leq data for the first ten days of the lockdown period (equivalent to the first ten days of the new year) at Shohada. As shown in Fig 10 the RF model's prediction indicate that the lockdown had a relatively small impact on noise pollution levels in this station in Mashhad. The forecasted values for the first ten days closely reflect the observed data pattern during that period. Quantifying this effect, the average Leq forecast for this period was 73.09 dB, only 3.30% higher than the average of the observed data (70.75 dB). The predicted Leq values ranged from 67.85 dB to 75.20 dB, closely matching the observed range of 63.60 dB to 76.28 dB.

Comparison with other machine learning models

The performance of the RF model utilized in this study to predict noise pollution levels in Mashhad, Iran, was compared to results from similar studies using different machine learning models Table 7. These studies examined noise prediction in various locations worldwide, including the New Klang Valley, Malaysia^{35,66}, Quito, Ecuador⁴⁰, and Nicosia, Northern Cyprus⁶⁷. Table 7 summarizes the performance measures reported in these studies, including R^2 , RMSE, and MAE.

As shown in Table 7 R^2 values for various models in different studies range from 0.1894 to 0.914. The RF model in this study obtained the highest R-square value (0.914) compared to the models used in other places. This indicates a strong positive correlation between forecasted and observed Leq in Mashhad using this model. The reported RMSE values ranged from 0.1177 and 5.589. The RMSE of the RF model (0.967) was within this

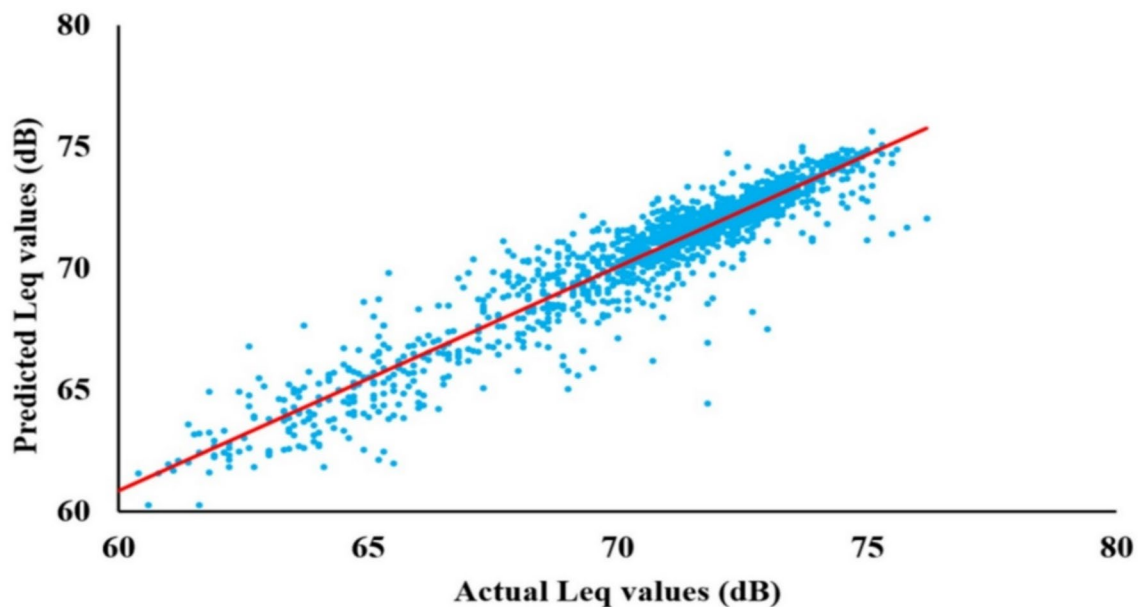


Fig. 9. Scatter plot of actual vs. predicted values for random forest model predictions on the same validation subset used for performance evaluation.

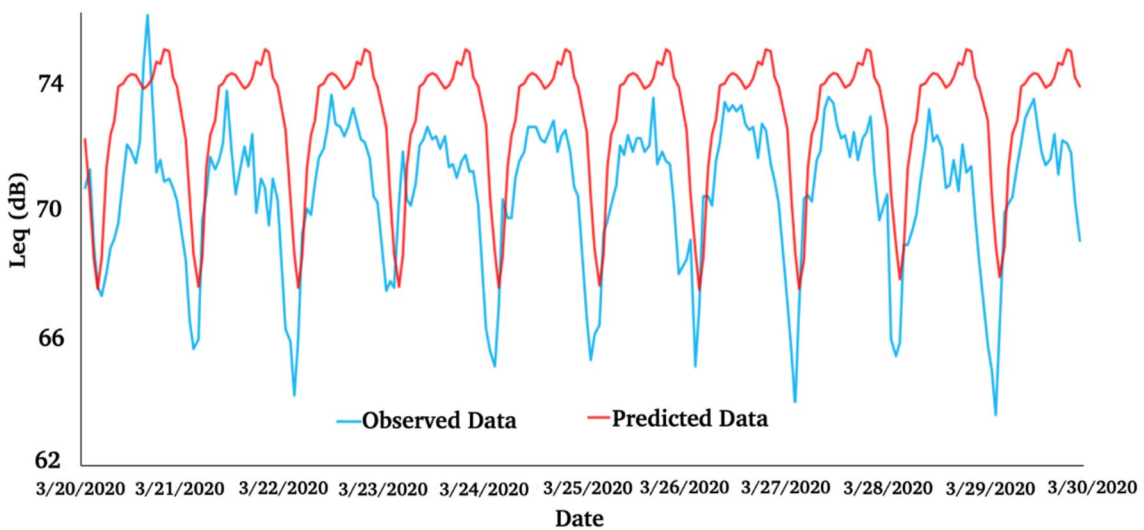


Fig. 10. Comparison of random forest model predictions with actual data during the initial ten days of the lockdown in shohada station in Mashhad.

range, which indicates a reasonable level of accuracy in forecasting Leq. Similarly, reported MAE values ranged from 0.620 to 4.46, with the RF model's MAE (0.620) showing its ability to predict Leq with a mean absolute error of 0.62 dB.

Beyond its predictive accuracy, a key advantage of the RF model lies in its efficient performance, characterized by lower computational costs and reduced data requirements, especially when compared to neural network models^{1,68}. This makes RF a practical and robust choice for noise prediction tasks. The ensemble-based structure of the RF model helps sustain high predictive accuracy even with smaller datasets, as it demonstrates reduced susceptibility to overfitting. Moreover, the model requires fewer hyperparameters and less intensive tuning, which significantly decreases training time and computational resource needs.

These benefits are particularly valuable in real-time prediction scenarios, where rapid processing of sensor or field data is crucial. The RF model can efficiently handle incoming data streams, providing reliable insights in dynamic environments—an essential feature for applications like noise level forecasting. Its ability to generate fast and accurate predictions with modest data requirements underscores its practical utility.

Area	Model*	R ²	RMSE	MAE	Reference
New Klang Valley, Shah Alam, Malaysia	RF	0.90	4.47	3.86	Adulaimi et al. (2021) ³⁵
	SVM	0.88	4.89	4.30	
	DT	0.88	4.83	4.26	
	LR	0.88	4.79	4.46	
New Klang Valley, Shah Alam, Malaysia	ANN	0.707	5.589	-	Ahmed et al. (2021) ⁶⁶
	CFS-ANN	0.688	3.272	-	
	Ensemble RF-ANN	0.835	2.378	-	
Quito, Ecuador	MLR	0.1968	2.6554	-	Bravo-Moncayo et al. (2019) ⁴⁰
	SVM	0.1894	2.4914	-	
	ANN	0.3263	1.9133	-	
Nicosia city, North Cyprus	FFNN	0.7840	0.1492	-	Nourani et al. (2020) ⁶⁷
	ANFIS	0.8670	0.1177	-	
	SVR	0.7633	0.1570	-	
	MLR	0.6607	0.1880	-	
Mashhad, Iran	RF	0.914	0.967	0.620	This study

Table 7. An overview of analogous studies and their respective validation outcomes in forecasting noise levels. *RF: Random forest, SVM: Support vector machine, DT: Decision Tree, LR: Linear regression, ANN: Artificial neural network, CFS-ANN: Correlation-based feature selection with artificial neural network, MLR: Multiple linear regression, FFNN: Feed forward neural network, ANFIS: Adaptive Neuro Fuzzy Inference System. A dash (-) indicates that the study did not include a particular metric in its analysis

Although deep neural networks may excel with very large or highly complex datasets, the RF model offers an effective balance between performance and efficiency⁶⁹. This balance makes it especially suitable for small to medium-sized datasets, as demonstrated in the noise prediction tasks of this study. This study demonstrates that the RF model proves to be an efficient approach to investigating noise dynamics in local case studies. Although not aiming for global generalization, it is useful in providing insights for policy considerations, such as quarantines, that influence urban noise patterns. Due to the dataset's small size and restricted geographical scope, the findings should be interpreted with caution and considered primarily as exploratory results in the specific context of this regional case study.

Comparing models from different studies directly can be challenging. This results from variations in factors such as data collection methods, data quality, and reported performance measures. However, considering the range of values observed in other studies, the performance of the RF model in this study highlights its effectiveness in predicting Leq in Mashhad. These findings suggest that machine learning can support dynamic noise monitoring and guide evidence-based urban planning beyond the COVID-19 pandemic. The COVID-19 quarantine in Iran provided a unique opportunity to study urban noise dynamics under significantly reduced human activity, providing insights for future urban noise management. The clear link between reduced human activity and lower Leq indicates that urban planning can significantly reduce noise pollution even in normal conditions. These strategies include increasing public transport, developing pedestrian-only zones, and promoting active modes of transport to reduce the use of private vehicles. These results support the adoption of the low-traffic or car-free policies in crowded commercial and residential zones, as well as further efforts to encourage sustainable mobility options, including walking, cycling, and electric vehicles.

Additionally, the growing popularity of remote and hybrid work suggested a possible way to reduce Leq during peak hours that cities might incorporate into long-term mobility planning. Urban green infrastructure, including vegetative noise barriers and expanded green spaces can also reduce noise while improving air quality, thermal comfort, and mental health.

Furthermore, the successful application of the RF model in this study shows how machine learning facilitates dynamic, data-driven noise monitoring and policy development. These tools can help urban managers identify noise hotspots and deploy targeted, evidence-based interventions. Together, these insights provide a strong foundation for designing cities that are not only quieter and healthier, but also more resilient to future disruptions.

Limitation of the study

Although this research offers useful information on how the COVID-19 lockdown affected noise pollution levels in Mashhad's main intersections, it is important to acknowledge several limitations. First, the analysis is based on data collected from fixed monitoring stations, which might not accurately represent noise fluctuations in all areas of the city. Although the current study may not fully represent residential, industrial, or suburban areas, it provides a solid foundation for understanding the dynamics of short-term urban noise. We suggest that the monitoring network be expanded in the future research to include a wider range of land use types. Moreover, the study period is relatively short, limited to March 21–April 20, 2019, and March 20–April 19, 2020 which may not fully reflect long-term trends or seasonal changes in noise pollution. This limitation was due to challenges such as equipment failures, inadequate infrastructure, and lack of pre-pandemic data for specific stations. These challenges were exacerbated by geopolitical barriers that limited access to advanced monitoring equipment. Furthermore, while the Wilcoxon signed-rank test and the RF model provide adequate statistical analyses, the

analysis does not explicitly consider other factors impacting Leq like shifts in traffic patterns, weather conditions, and human behavior. Finally, the findings of this case study may not directly generalizable to other urban areas or regions with different urban characteristics or lockdown measures. Despite these limitations, this study highlights the significance of improving infrastructure and developing international collaborations to improve long-term data collection efforts.

Conclusion

This study investigated how human activities affect noise pollution in Mashhad by studying the short-term noise level fluctuation at key intersections during the COVID-19 lockdown. A two-pronged approach was deployed. Initially, a statistical analysis was performed to compare the Leq data obtained during the pre-lockdown (March 21-April 20, 2019) and lockdown (March 20-April 19, 2020) periods using the Wilcoxon signed-rank test. The analysis revealed a significant but modest impact of COVID-19 restrictions, particularly traffic limitations, on Leq in Mashhad. Our finding reveals that while Leq in Mashhad decreased during lockdown, the reduction was less pronounced compared to other regions. This demonstrate the impact of regional variables such as climatic conditions, vegetation cover, vehicle speed and type, asphalt quality, road width, and slope, and the number of speed bumps on the way environmental noise reacts to social disruptions.

Additionally, a predictive model utilizing a RF was developed to analyze localized patterns in urban noise dynamics. The RF model achieved a high R^2 value (0.914), showing a significant positive relationship between forecasted and observed Leq. The model's RMSE and MAE values (0.967 and 0.620, respectively) underscores the utility of machine learning techniques for understanding urban noise in a defined setting. Although our model is not designed for broad generalization, it establishes a reliable baseline for measuring noise deviation during the lockdown. Such insight is useful for localized noise management efforts as well as the future studies.

In conclusion, this study demonstrated that human activities play a major role in contributing to noise pollution in Mashhad. The findings emphasize the potential advantages of urban planning strategies that reduce traffic and noise generation.

Data availability

The authors confirm that all data and materials support their published claims and comply with standards. Data will be made available on request. Requests for data should be directed to Mitra Mohammadi at mitramohammadi@gmail.com.

Received: 11 November 2024; Accepted: 13 November 2025

Published online: 11 December 2025

References

1. Temtem, F. Soundscapes between the music of the city and the urban noise. *Arte Imagen y Sonido* **2**, 74–95. <https://doi.org/10.33064/3ais3519> (2022).
2. Bala, M. & Verma, D. Investigation & examination of noise pollution—definition, sources, effects, monitoring and control. *Int. J. Soc. Sci.* **10**, 182–207. <https://doi.org/10.2139/ssrn.3640509> (2020).
3. Patel, R., Singh, P. K. & Saw, S. Traffic Noise Modeling under Mixed Traffic Condition in Mid-Sized Indian City: A Linear Regression and Neural Network-Based Approach. *Int J Mathematical Eng Manag Sci* **9**(3), 411–434 (2024).
4. Morillas, J. M. B., Gozalo, G. R., González, D. M., Moraga, P. A. & Vilchez-Gómez, R. Noise pollution and urban planning. *Current Pollution Reports* **4**(3), 208–219 (2018).
5. Buxton, R. T., Pearson, A. L., Allou, C., Fristrup, K. & Wittemyer, G. A synthesis of health benefits of natural sounds and their distribution in national parks. *Proc. Natl. Acad. Sci. USA* **118**, e2013097118 (2021).
6. Alimohammadi, I., Kanrash, F. A., Abolghasemi, J., Vosoughi, S. & Chalak, M. H. Relationship between noise annoyance and cognitive performance in automotive workers exposed to chronic noise. *J. UOEH* **41**, 375–385. <https://doi.org/10.7888/juoh.41.375> (2019).
7. Araújo Alves, J., Neto Paiva, F., Torres Silva, L. & Remaldo, P. Low-frequency noise and its main effects on human health—A review of the literature between 2016 and 2019. *Appl. Sci.* **10**, 5205. <https://doi.org/10.3390/app10155205> (2020).
8. Hahad, O. et al. Cerebral consequences of environmental noise exposure. *Environ. Int.* **165**, 107306. <https://doi.org/10.1016/j.envint.2022.107306> (2022).
9. Thompson, R. et al. Noise pollution and human cognition: An updated systematic review and meta-analysis of recent evidence. *Environ. Int.* **158**, 106905. <https://doi.org/10.1016/j.envint.2021.106905> (2022).
10. Mishra, A., Das, S., Singh, D. & Maurya, A. K. Effect of COVID-19 lockdown on noise pollution levels in an Indian city—a case study of Kanpur. *Environ. Sci. Pollut. Res.* **28**, 46007–46019 (2021).
11. Tiwari, S. K., Kumaraswamidhas, L. A. & Garg, N. Assessment of noise pollution and associated subjective health complaints in Jharia Coalfield, India: A structural equation model analysis. *Noise Mapping* **10**(1), 20220172 (2023).
12. Patel, R., Singh, P. K., Saw, S. & Tiwari, S. Assessment and prediction of noise pollution-induced health impacts in urban environment: a structural equation modeling (SEM)-based approach. *Arab. J. Geosci.* **17**(11), 1–17 (2024).
13. Patel, R., Singh, P. K. & Saw, S. A modeling approach for suitability evaluation of traffic noise prediction under mixed traffic situation in mid-sized Indian cities. *Innovative Infrastructure Solutions* **9**(6), 183 (2024).
14. Perez, O. A., Delina, L. L. & Steuer, B. Behavioural responses to the COVID-19 pandemic and their implications for Sustainable Development Goals in Hong Kong. *Cities Health.* **8**(2), 226–239. <https://doi.org/10.1080/23748834.2024.2303566> (2024).
15. Moezzi, S. M., Mohammadi, M., Mohammadi, M., Saloglu, D. & Sheikhholeslami, R. Machine learning insights into PM2.5 changes during COVID-19 lockdown: LSTM and RF analysis in Mashhad. *Environ. Monit. Assess.* **196**(5), 453 (2024).
16. Sohrabi, S. et al. Health impacts of COVID-19 through the changes in mobility. *Sustainability* **15**, 4095. <https://doi.org/10.3390/su15054095> (2023).
17. Lee, K. S. & Eom, J. K. Systematic literature review on impacts of COVID-19 pandemic and corresponding measures on mobility. *Transp* <https://doi.org/10.1007/s11116-023-10392-2> (2023).
18. Zhang, Z. et al. COVID-19, traffic demand, and activity restriction in China: A national assessment. *Travel Behav. Soc.* **31**, 10–23. <https://doi.org/10.1016/j.tbs.2022.11.001> (2023).
19. Helmi, A. A., Romli, M. H. & Ezani, E. Influence of COVID-19 lockdown on noise level reduction: A scoping review with stakeholders' consultation. *MJMHS* <https://doi.org/10.47836/mjmhs.19.s14.16> (2023).

20. Asensio, C., Pavón, I. & De Arcas, G. Changes in noise levels in the city of Madrid during COVID-19 lockdown in 2020. *J. Acoust. Soc. Am.* **148**(3), 1748–1755. <https://doi.org/10.1121/10.0002008> (2020).
21. Terry, C., Rothandler, M., Zipf, L., Dietze, M. C. & Primack, R. B. Effects of the COVID-19 pandemic on noise pollution in three protected areas in metropolitan Boston (USA). *Biol. Conserv.* **256**, 109039. <https://doi.org/10.1016/j.biocon.2021.109039> (2021).
22. Aumond, P., Can, A., Lagrange, M., Gontier, F. & Lavandier, C. Multidimensional analyses of the noise impacts of COVID-19 lockdown. *J. Acoust. Soc. Am.* **151**(2), 911–923. <https://doi.org/10.1121/10.0009324> (2022).
23. Joshi, K. K. & Pokhriyal, E. A. Impact of coronavirus on noise pollution in the Himalayan city of Dehradun: A case study. *Res. Rev. Res. J. Biol.* **9**, 3 (2021).
24. Basu, B. et al. Investigating changes in noise pollution due to the COVID-19 lockdown: The case of Dublin. *Ireland. Sustain. Cities Soc.* **65**, 102597. <https://doi.org/10.1016/j.scs.2020.102597> (2021).
25. Rumpel, R., Venkataraman, S. & Göransson, P. Noise measurements as a proxy to evaluating the response to recommendations in times of crisis: An update analysis of the transition to the second wave of the COVID-19 pandemic in Central Stockholm. *Sweden. J. Acoust. Soc. Am.* **149**(3), 1838–1842. <https://doi.org/10.1121/10.0003778> (2021).
26. Munoz, P. et al. Lockdown during COVID-19 pandemic: Impact on road traffic noise and on the perception of sound environment in France. *Noise Mapp.* **7**(1), 287–302. <https://doi.org/10.1515/noise-2020-0024> (2020).
27. Romina, I., Jafari, M. & Kalhor, M. Investigating geopolitical factors of religious cities (case study: Mashhad City). *PalArch's J. Archaeol. Egypt/Egyptol.* **18**, 3342–3363 (2021).
28. Gheibi, M., Karrabi, M., Latifi, P. & Fathollahi-Fard, A. M. Evaluation of traffic noise pollution using geographic information system and descriptive statistical method: A case study in Mashhad Iran. *Environ. Sci. Pollut. Res.* <https://doi.org/10.1007/s11356-022-18532-4> (2022).
29. Ulloa, J. S. et al. Listening to cities during the COVID-19 lockdown: How do human activities and urbanization impact soundscapes in Colombia? *Biol. Conserv.* **255**, 108996. <https://doi.org/10.1016/j.biocon.2021.108996> (2021).
30. Caraka, R. E. et al. Did noise pollution really improve during COVID-19? Evidence from Taiwan. *Sustainability* **13**, 5946. <https://doi.org/10.3390/su13115946> (2021).
31. Velastegui-Montoya, A. et al. Acoustic contamination assessment during the transition between the COVID-19 restrictions and reactivation: An exploratory analysis in Guayaquil. *Geogr. Sustain.* **4**(2), 138–149. <https://doi.org/10.1016/j.geosus.2023.02.001> (2023).
32. Baqar, M. et al. Noise pollution in the hospital environment of a developing country: A case study of Lahore (Pakistan). *Arch. Environ. Occup. Health.* **73**(6), 367–374. <https://doi.org/10.1080/19338244.2018.1428634> (2018).
33. Casla-Herguedas, B., Romero-Fernández, A., Carrascal, T., Navas-Martín, M. Á. & Cuerdo-Vilches, T. Noise perception and health effects on population: A cross-sectional study on COVID-19 lockdown by noise sources for Spanish dwellings. *Buildings* **13**(9), 2224. <https://doi.org/10.3390/buildings13092224> (2023).
34. Lenzi, S., Sádaba, J. & Lindborg, P. Soundscape in times of change: Case study of a city neighbourhood during the COVID-19 lockdown. *Front. psychol.* **12**, 570741. <https://doi.org/10.3389/fpsyg.2021.570741> (2021).
35. Adulaimi, A. A. A., Pradhan, B., Chakraborty, S. & Alamri, A. Traffic noise modelling using land use regression model based on machine learning, statistical regression and GIS. *Energies* **14**, 5095. <https://doi.org/10.3390/en14165095> (2021).
36. Liu, Y. et al. Comparison of land use regression and random forests models on estimating noise levels in five Canadian cities. *Environ. Pollut.* **256**, 113367. <https://doi.org/10.1016/j.envpol.2019.113367> (2020).
37. Liu, Y. et al. Integrating random forests and propagation models for high-resolution noise mapping. *Environ. Res.* **195**, 110905. <https://doi.org/10.1016/j.envres.2021.110905> (2021).
38. Baffoe, P. E. & Boye, C. B. Performance Evaluation of Extreme Learning Machine Techniques for Prediction of Noise Pollution. *Ghana. Min. J.* **24**(1), 66–74 (2024).
39. Rehman, M. U., Kamal, M. & Tiwari, S. K. Statistical analysis based on a two-staged SEM-SVM approach for environmental noise annoyance prediction and identification of influencing factors. *Int. J. Hum. Cap. Urban. Manage.* **10**(1), 121–134. <https://doi.org/10.22034/IJHCUM.2025.01.08> (2025).
40. Bravo-Moncayo, L., Lucio-Naranjo, J., Chávez, M., Pavón-García, I. & Garzón, C. A machine learning approach for traffic-noise annoyance assessment. *Appl. Acoust.* **156**, 262–270. <https://doi.org/10.1016/j.apacoust.2019.07.010> (2019).
41. Fan, Z. & Signorelli, V. Is the noise still going on? Predicting repeat noise complaints with historical time course and random forest classifiers. *Environ. Plan. B: Urban. Anal. City. Sci.* **51**(2), 496–511. <https://doi.org/10.1177/23998083231184254> (2024).
42. Ren, X., Mi, Z. & Georgopoulos, P. G. Socioexposomics of COVID-19 across New Jersey: a comparison of geostatistical and machine learning approaches. *J. Expo. Sci. Environ. Epidemiol.* **34**(2), 197–207. <https://doi.org/10.1038/s41370-023-00518-0> (2024).
43. Manzella, F., Pagliarini, G., Sciaivico, G. & Stan, I. E. (2021) Interval temporal random forests with an application to COVID-19 diagnosis. In *28th International Symposium on Temporal Representation and Reasoning (TIME 2021)*. Schloss Dagstuhl-Leibniz-Zentrum für Informatik.
44. Das, C. P., Swain, B. K., Goswami, S. & Das, M. Prediction of traffic noise induced annoyance: A two-staged SEM-Artificial Neural Network approach. *Transp. Res. D: Transp. Environ.* **100**, 103055. <https://doi.org/10.1016/j.trd.2021.103055> (2021).
45. Miri, M. et al. Mortality and morbidity due to exposure to outdoor air pollution in Mashhad metropolis. *Iran. The AirQ model approach. Environ. Res.* **151**, 451–457. <https://doi.org/10.1016/j.envres.2016.07.039> (2016).
46. Rumpel, R., Venkataraman, S. & Göransson, P. An observation of the impact of CoViD-19 recommendation measures monitored through urban noise levels in central Stockholm. *Sweden. Sustainable Cities and Society* **63**, 102469. <https://doi.org/10.1016/j.jscs.2020.102469> (2020).
47. Hornberger, J. et al. Impact of the COVID-19 lockdown measures on noise levels in urban areas—A pre/during comparison of long-term sound pressure measurements in the Ruhr Area, Germany. *Int. J. Environ. Res. Public Health* **18**(9), 4653. <https://doi.org/10.3390/ijerph18094653> (2021).
48. U.S. Environmental Protection Agency. Information on levels of environmental noise requisite to protect public health and welfare with an adequate margin of safety (Report No. 550/9-74-004). U.S. Government Printing Office. <https://nepis.epa.gov/Exe/ZyPU RL.cgi?Dockey=2000L3LN.TXT> (1974).
49. International Organization for Standardization. ISO 1996-2:2017 Acoustics — Description, measurement and assessment of environmental noise — Part 2: Determination of sound pressure levels. <https://www.iso.org/standard/59766.html> (2017).
50. Gonzalez, D. M., Morillas, J. M. B., Gozalo, G. R. & Godinho, L. Evaluation of exposure to road traffic noise: Effects of microphone height and urban configuration. *Environ. Res.* **191**, 110055 (2020).
51. Hollander, M., Wolfe, D. A. & Chicken, E. Nonparametric Statistical Methods (3rd Edition). *Wiley* (2013).
52. Gong, H., Sun, Y., Shu, X. & Huang, B. Use of random forests regression for predicting IRI of asphalt pavements. *Constr. Build. Mater.* **189**, 890–897. <https://doi.org/10.1016/j.conbuildmat.2018.09.017> (2018).
53. Jog, A., Carass, A., Roy, S., Pham, D. L. & Prince, J. L. Random forest regression for magnetic resonance image synthesis. *Med. Image. Anal.* **35**, 475–488. <https://doi.org/10.1016/j.media.2016.08.009> (2017).
54. Ding, W. & Qie, X. Prediction of air pollutant concentrations via RANDOM forest regressor coupled with uncertainty analysis—A case study in Ningxia. *Atmosphere* **13**(6), 960. <https://doi.org/10.3390/atmos13060960> (2022).
55. Alsouda, Y., Plana, S. & Kurti, A. Iot-based urban noise identification using machine learning: performance of SVM, KNN, bagging, and random forest. In *Proceedings of the international conference on omni-layer intelligent systems*. 62–67 (2019). <https://doi.org/10.1145/3312614.3312631>

56. Vijayalakshmi, A., Rubi, J., Dhivya, J.A. & AS, A.R. Machine Learning-Based Prediction and Analysis of Air and Noise Pollution in Urban Environments. In *2024 2nd International Conference on Sustainable Computing and Smart Systems (ICSCSS)*. 1080–1085. IEEE (2024). <https://doi.org/10.1109/ICSCSS60660.2024.10625644>
57. Vinutha, H.P., Poornima, B. & Sagar, B.M. Detection of outliers using interquartile range technique from intrusion dataset. In *Information and decision sciences: Proceedings of the 6th international conference on ficta*. 511–518 (2018). Springer Singapore. https://doi.org/10.1007/978-981-10-7563-6_53
58. Dowlatabadi, Y., Abadi, S., Sarkhosh, M., Mohammadi, M. & Moezzi, S. M. M. Assessing the impact of meteorological factors and air pollution on respiratory disease mortality rates: a random forest model analysis (2017–2021). *Sci. Rep.* **14**(1), 24535. <https://doi.org/10.1038/s41598-024-74440-2> (2024).
59. Emamjomeh, M. M., Nikpay, A. & Variani, S. A. study of noise pollution in Qazvin (2010). *J. Inflamm. Dis.* **15**, 63–70 (2011).
60. Moasher, N., Monazzam Esmaeelpoore, M. R., Abolhasannejad, V., Abbaszadeh, M. & Movahedi, E. Assessment of noise pollution indices in Birjand old districts in 2010. *J. Birjand Univ. Med. Sci.* **19**, 439–447 (2012).
61. Yari, A. R. et al. Evaluation of traffic noise pollution and control solutions offering: A case study in Qom. *Iran. J. Sabzevar Univ. Med. Sci.* **23**, 600–607 (2016).
62. Aletta, F. et al. Analysing urban traffic volumes and mapping noise emissions in Rome (Italy) in the context of containment measures for the COVID-19 disease. *Noise Mapp.* **7**(1), 114–122. <https://doi.org/10.1515/noise-2020-0010> (2020).
63. Maggi, A. L. et al. Perception of the acoustic environment during COVID-19 lockdown in Argentina. *J. Acoust. Soc. Am.* **149**(6), 3902–3909. <https://doi.org/10.1121/10.0005131> (2021).
64. Alsina-Pagès, R. M., Bergadà, P. & Martínez-Suquía, C. Changes in the soundscape of Girona during the COVID lockdown. *J. Acoust. Soc. Am.* **149**(5), 3416–3423. <https://doi.org/10.1121/10.0004986> (2021).
65. Rodríguez, R., Machimbarrena, M. & Tarrero, A. I. Environmental noise evolution during COVID-19 state of emergency: Evidence of Peru's need for action plans. *Acoustics.* **4**(2), 479–491. <https://doi.org/10.3390/academics4020030> (2022).
66. Ahmed, A. A., Pradhan, B., Chakraborty, S. & Alamri, A. Developing vehicular traffic noise prediction model through ensemble machine learning algorithms with GIS. *Arab. J. Geosci.* **14**, 1–14. <https://doi.org/10.1007/s12517-021-08114-y> (2021).
67. Nourani, V., Gökçekuş, H. & Umar, I. K. Artificial intelligence based ensemble model for prediction of vehicular traffic noise. *Environ. Res.* **180**, 108852. <https://doi.org/10.1016/j.envres.2019.108852> (2020).
68. Probst, P., Wright, M. N. & Boulesteix, A. L. Hyperparameters and tuning strategies for random forest. *Wiley Interdiscip Rev. Data Min. Knowl. Discov.* **9**, e1301 (2019).
69. Rodriguez-Galiano, V., Sanchez-Castillo, M., Chica-Olmo, M. & Chica-Rivas, M. J. O. G. R. Machine learning predictive models for mineral prospectivity: An evaluation of neural networks, random forest, regression trees and support vector machines. *Ore Geol. Rev.* **71**, 804–818 (2015).

Author contributions

All authors contributed to the study's conception and design. Raheleh Valizadeh Ardalan: conceptualization, methodology, modeling, writing- original draft. Mitra Mohammadi: supervision, conceptualization, methodology, writing- the original draft, editing. Mohammad Sadegh Bahadari: supervision, conceptualization, writing- original draft, editing. Mandana Mohammadi: methodology, modeling, writing- original draft, software. Seyed Mohammad Mahdi Moezzi: methodology, modeling, writing- original draft, software. Didem Saloglu: conceptualization, methodology, writing- original draft, editing.

Declarations

Competing interests

The authors declare no competing interests.

Ethics approval

All authors have read, understood, and have complied as applicable with the statement on the “Ethical responsibilities of Authors” as found in the Instructions for Authors. This article does not contain any studies with human/animal participants performed by any of the authors.

Consent to participate

All the authors gave their consent to participate.

Additional information

Supplementary Information The online version contains supplementary material available at <https://doi.org/10.1038/s41598-025-29011-4>.

Correspondence and requests for materials should be addressed to M.M. or D.S.

Reprints and permissions information is available at www.nature.com/reprints.

Publisher's note Springer Nature remains neutral with regard to jurisdictional claims in published maps and institutional affiliations.

Open Access This article is licensed under a Creative Commons Attribution-NonCommercial-NoDerivatives 4.0 International License, which permits any non-commercial use, sharing, distribution and reproduction in any medium or format, as long as you give appropriate credit to the original author(s) and the source, provide a link to the Creative Commons licence, and indicate if you modified the licensed material. You do not have permission under this licence to share adapted material derived from this article or parts of it. The images or other third party material in this article are included in the article's Creative Commons licence, unless indicated otherwise in a credit line to the material. If material is not included in the article's Creative Commons licence and your intended use is not permitted by statutory regulation or exceeds the permitted use, you will need to obtain permission directly from the copyright holder. To view a copy of this licence, visit <http://creativecommons.org/licenses/by-nc-nd/4.0/>.

© The Author(s) 2025